# Electrical Impedance Tomography and Biomedical Applications

Eung Je Woo

Department of Biomedical Engineering, Kyung Hee University, Korea, ejwoo@khu.ac.kr

**Abstract**: Two impedance imaging systems of multi-frequency electrical impedance tomography (MFEIT) and magnetic resonance electrical impedance tomography (MREIT) are described. MFEIT utilizes boundary measurements of current-voltage data at multiple frequencies to reconstruct cross-sectional images of a complex conductivity distribution ($\sigma + i\omega\varepsilon$) inside the human body. The inverse problem in MFEIT is ill-posed due to the nonlinearity and low sensitivity between the boundary measurement and the complex conductivity. In MFEIT, we therefore focus on time- and frequency-difference imaging with a low spatial resolution and high temporal resolution. Multi-frequency time- and frequency-difference images in the frequency range of 10 Hz to 500 kHz are presented. In MREIT, we use an MRI scanner to measure an internal distribution of induced magnetic flux density subject to an injection current. This internal information enables us to reconstruct cross-sectional images of an internal conductivity distribution with a high spatial resolution. Conductivity image of a postmortem canine brain is presented and it shows a clear contrast between gray and white matters. Clinical applications for imaging the brain, breast, thorax, abdomen, and others are briefly discussed.

**Keywords**: complex conductivity, image reconstruction, EIT, MREIT.

## 1. INTRODUCTION

For a biological tissue, its electrical conductivity ($\sigma$) and permittivity ($\varepsilon$) are affected by molecular composition, cellular structure, membrane properties, concentration and mobility of ions in intra- and extra-cellular fluids, frequency and amplitude of measuring current, temperature, and other factors. Noticing the abundance of information embedded in the complex conductivity ($\sigma + i\omega\varepsilon$) values of different tissues, there have been numerous research works in the impedance imaging area to visualize distributions of $\sigma$ and $\omega\varepsilon$ inside the human body as cross-sectional images. Information about the complex conductivity distribution is of significant importance in many biomedical applications including modeling of tissues in bioelectricity, estimation of internal current density distributions, diagnosis of physiological functions, cancerous lesion detections, and so on (Holder 2005).In order to extract information about internal conductivity and permittivity distributions, we may inject current into the human body through surface electrodes. The injection current induces voltage, current density, and magnetic flux density distributions and these are determined by the geometry, electrode configuration, and complex conductivity distribution of the imaging object. In multi-frequency electrical impedance tomography (MFEIT), we utilize measured current-voltage data on the boundary to provide cross-sectional images of a complex conductivity distribution. Mathematical analysis of this imaging problem indicates that it has fundamental limitations due to the ill-posed nature of the corresponding inverse problem. Therefore, time- and frequency-difference image

reconstructions are more practical in MFEIT. Describing a new MFEIT system with a bandwidth of 10 Hz to 500 kHz, we present typical time- and frequency-difference images.

Magnetic resonance electrical impedance tomography (MREIT) has been suggested to overcome the ill-posedness of the image reconstruction problem in EIT. The key idea is to utilize the internal magnetic flux density data measured by using an MRI scanner. After introducing a 3 Tesla MREIT system, we will present experimental data and reconstructed conductivity image with much better spatial resolution and accuracy. Summarizing latest outcomes of the MFEIT and MREIT research, we will discuss future research directions of the imaging techniques.

## 2. MULTI-FREQUENCY ELECTRICAL IMPEDANCE TOMOGRAPHY

### 2.1 Problem Formulation

We denote the three-dimensional imaging object with a complex conductivity distribution ($\sigma + i\omega\varepsilon$) as $\Omega$ with its boundary $\partial\Omega$. When we inject sinusoidal current $i(t) = I\sin(\omega t)$ in ampere through a pair of surface electrodes, it induces a distribution of voltage $v(\mathbf{r}, t) = V(\mathbf{r})\sin(\omega t + \theta(\mathbf{r}))$ in volt at a position $\mathbf{r}$ throughout the domain $\Omega$. Using the phasor notation, the voltage at $\mathbf{r}$ can be expressed as $\mathbf{V}(\mathbf{r}) = V(\mathbf{r})\angle\theta(\mathbf{r}) = V(\mathbf{r})\sin\theta(\mathbf{r}) + iV(\mathbf{r})\cos\theta(\mathbf{r})$, When the frequency is relatively low, it satisfies the following elliptic partial differential equation:

$$\begin{cases} \nabla\cdot\left(\left(\sigma(\mathbf{r},\omega)+i\omega\varepsilon(\mathbf{r},\omega)\right)\nabla\mathbf{V}(\mathbf{r},\omega)\right)=0 & \text{in } \Omega \\ -\left(\sigma(\mathbf{r},\omega)+i\omega\varepsilon(\mathbf{r},\omega)\right)\nabla\mathbf{V}(\mathbf{r},\omega)\cdot\mathbf{n}=g & \text{on } \partial\Omega \end{cases} \tag{1}$$

where $\mathbf{n}$ is the outward unit normal vector on $\partial\Omega$ and $g$ the magnitude of the current density on $\partial\Omega$ due to the injection current.

In most biomedical applications, the voltage data are measurable only on a limited number electrodes placed on the boundary $\partial\Omega$. Then, the difference image reconstruction problem in MFEIT is to find changes in $\sigma$ and $\omega\varepsilon$ from measured data of $\mathbf{V}(\mathbf{r},\omega)$ on those surface electrodes. When $\sigma$ and $\omega\varepsilon$ change with time due to physiological functions or pathological status of tissues, we may obtain two sets of complex boundary voltage data subject to the same injection current at time $T_1$ and $T_2$ and then the voltage difference between $T_1$ and $T_2$ can be used for time-difference image reconstructions of $\sigma$ and $\omega\varepsilon$. If $\sigma$ and $\varepsilon$ change with frequency, we obtain two sets of complex boundary voltage data at two difference frequencies of $\omega_1$ and $\omega_2$ at the same time instant. The voltage difference between $\omega_1$ and $\omega_2$ can produce frequency-difference images of $\sigma$ and $\omega\varepsilon$. In this paper, we used a difference image reconstruction algorithm based on the sensitivity matrix (Lionheart *et al.* 2005).

### 2.2 MFEIT System and Imaging Experiments

Fig. 1 shows a recently developed MFEIT system called the KHU Mark1 (Oh *et al.*, 2007). It comprises four parts: (i) PC with USB ports and software, (ii) main body including one current source and multiple voltmeters, (iii) isolated dc power supply, and (iv) calibrator. The main

body is the core of the system and it includes a main controller, an intra-network controller on a digital backplane, a balanced current source, multiple voltmeters, and switching circuits on an analog backplane. The number of voltmeters could be 8, 16 or 32.

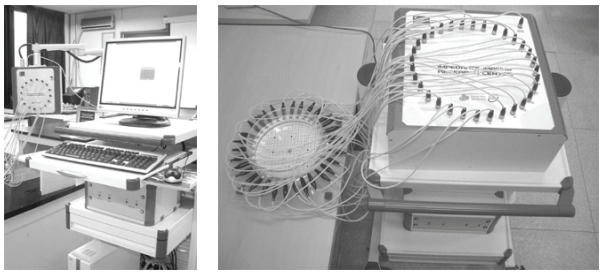

(a) (b)

**Fig. 1.** KHU Mark1 MFEIT system. (a) 16-channel and (b) 32-channel.

Voltmeters simultaneously acquire and demodulate differential voltage signals between pairs of electrodes. Major features of the system include a digital waveform generator, Howland current generator with multiple generalized impedance converters (GIC), digital phase-sensitive demodulation, tri-axial cables, contact impedance measurement, data overflow detection, spike noise rejection, automatic gain control, and programmable data averaging. The KHU Mark1 system measures both in-phase and quadrature components of a complex voltage data. By using a script file describing an operating mode, system setup can be easily changed. With an operating frequency range of 10 Hz to 500 kHz and a flexible strategy for addressing electrodes, it can be adopted for numerous biomedical applications including imaging studies of the brain, breast, thorax, abdomen, and others. Oh *et al.* (2007) describes the details of the system development and its performance in terms of current source output impedance, common-mode rejection ratio, signal-to-noise ratio, linearity error, and reciprocity error.

For imaging experiments, we used a two-dimensional saline phantom with 200 mm diameter, 100 mm height, and 0.05 S/m background conductivity. As an imaging object, we used a banana (30 mm diameter and 50 mm length). Its conductivity was 0.01 S/m at 10 Hz and increased to 0.17 S/m at 500 kHz. For the data collection, we used a 16-channel KHU Mark1 MFEIT system with several chosen operating frequencies. Time- and frequency-difference images were produced using a difference image reconstruction algorithm based on the sensitivity matrix (Lionheart *et al.* 2005).

### 2.3 Difference Image Reconstructions

We acquired the first set of multi-frequency data from the homogeneous saline phantom. Placing the banana inside the phantom, we collected the second set of multi-frequency data. Using both data sets with the first one as the reference data, we reconstructed time-difference images at multiple frequencies (Fig. 2). Frequency-difference images were reconstructed using the second data set with the data at 100 Hz as the reference (Fig. 3). Interestingly, the real part image at 50 kHz does not show the banana and its contrast with respect to the background of 0.05 S/m is reversed in the images at 100 and 250 kHz. As expected, at low frequencies of 50

and 100 Hz, the imaginary part images do not show the banana object clearly. The frequency-difference images in Fig. 3 show that the banana object is distinguished at frequencies over 5 kHz when the reference data is at 100 Hz.

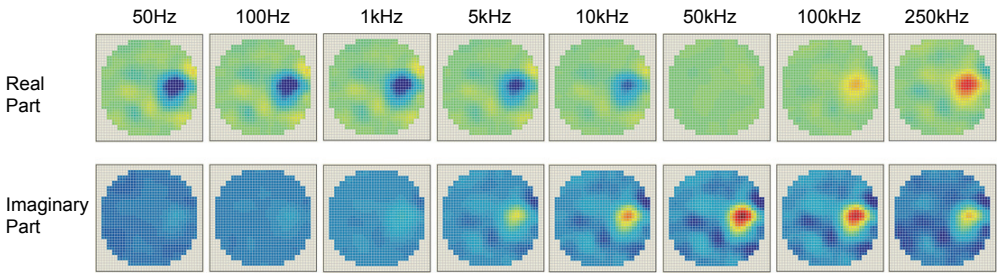


**Fig. 2.** Time-difference images of the banana object. Reference data was obtained from the homogeneous phantom at each frequency. All images at the same row are displayed with the same scale.

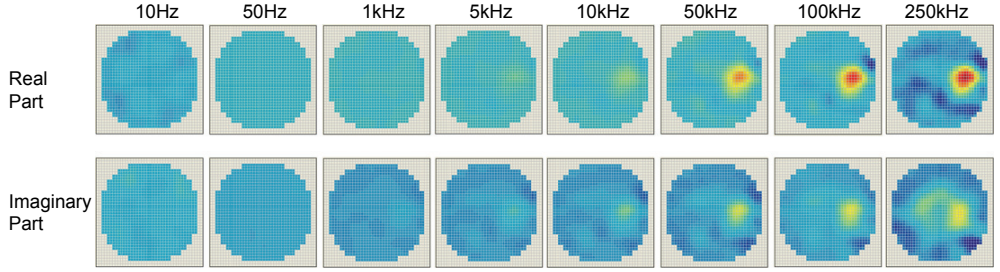


**Fig. 3.** Frequency-difference images of the banana object with the data at 100 Hz as the reference data. All images at the same row are displayed with the same scale.

## 3. MAGNETIC RESONANCE ELECTRICAL IMPEDANCE TOMOGRAPHY

### 3.1 Problem Formulation

Injection current into an electrically conducting object creates an internal current density distribution determined by the conductivity distribution of the object. The current density generates a magnetic flux density distribution following the Biot-Savart law. Utilizing measurements of internal magnetic flux densities induced by multiple injection currents, MREIT provides high-resolution conductivity images. In MREIT, we usually inject low-frequency current so that

$$\begin{cases} \nabla\cdot\left(\sigma(\mathbf{r})\nabla u(\mathbf{r})\right)=0 & \text{in } \Omega \\ -\sigma(\mathbf{r})\nabla u(\mathbf{r})\cdot\mathbf{n}=g & \text{on } \partial\Omega \end{cases} \tag{2}$$

where $u(\mathbf{r})$ is the induced voltage. The current density $\mathbf{J}$ inside $\Omega$ is

$$\mathbf{J}(\mathbf{r})=-\sigma(\mathbf{r})\nabla u(\mathbf{r}) \quad \text{in } \Omega \tag{3}$$

and the magnetic flux density $\mathbf{B}$ due to the current $\mathbf{J}$ in $\Omega$ is

$$\mathbf{B}(\mathbf{r})=\frac{\mu_0}{4\pi}\int_\Omega \mathbf{J}(\mathbf{r}')\times\frac{\mathbf{r}-\mathbf{r}'}{|\mathbf{r}-\mathbf{r}'|^3}d\mathbf{r}' \quad \text{in } \Omega\,. \tag{4}$$

We can see that the magnetic flux density **B** conveys information on the conductivity $\sigma$ via the current density **J**.

In order to measure the induced magnetic flux density inside Ω, we can use an MRI scanner. When we place an imaging object inside the MRI scanner with its main magnetic field in the $z$-direction, we can measure only the $z$-component $B_z$ of $\mathbf{B} = (B_x, B_y, B_z)$. Therefore, the conductivity image reconstruction problem in MREIT is to find the conductivity $\sigma$ from measured data of $B_z$ subject to multiple imaging currents (Woo *et al.* 2005).

### 3.2 MREIT System and Imaging Experiments

Fig. 4 shows a 3 Tesla MREIT system installed in the Impedance Imaging Research Center (IIRC), Kyung Hee University, Korea. It consists of a 3 Tesla MRI scanner, MREIT current source, and image reconstruction software. Numerous electrically conducting objects were used as imaging objects. In order to measure $B_z$ data inside the imaging object, the imaging current must be injected into the object in such a way that its timing is synchronized with an MRI pulse sequence. Obtaining $B_z$ data subject to multiple imaging currents with at least two different directions, we may use an conductivity image reconstruction algorithm such as the harmonic $B_z$ algorithm to produce high-resolution cross-sectional conductivity images (Woo *et al*. 2005).

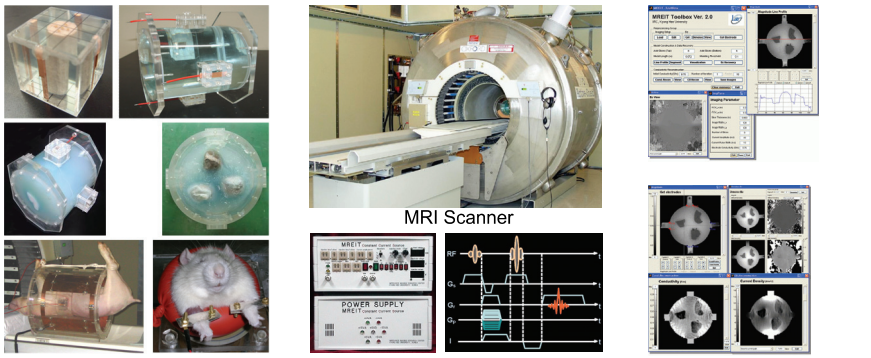


**Fig. 4.** 3 Tesla MREIT system.

### 3.3 Conductivity Images of Postmortem Canine Brains

Placing four recessed electrodes at four locations (dorsal, ventral and bilateral surfaces) on the head of a postmortem dog, we obtained an MR magnitude image of the canine head (Fig. 5(a)). Fig. 5(b) is the measured image of $B_z$ data subject to the horizontal imaging current. We reconstructed a cross-sectional conductivity image of the canine brain from the measured $B_z$ data using the harmonic $B_z$ algorithm as shown in Fig. 5(c).

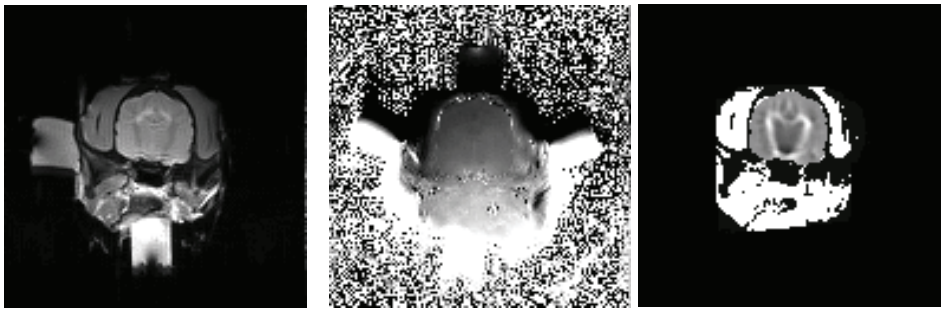

(a) (b) (c)

**Fig. 5.** (a) MR magnitude image, (b) magnetic flux density image, and conductivity image of the postmortem canine head.

## 4. DISCUSSION AND CONCLUSION

Impedance imaging modalities such as MFEIT and MREIT can be used to visualize physiological functions or status of the human body including respiration, cardiac circulation, brain function, stomach emptying, fracture healing, bladder filling, breast cancer diagnosis, and others. In MFEIT, better system developments and multi-frequency image reconstruction algorithms must be pursued to prove that its spatial and temporal resolution and accuracy are enough to distinguish any physiological difference of an organ or tissues with a diagnostic significance. Even though MREIT can provide high-resolution conductivity images, we must reduce the amplitude of the imaging current down to a level that the human subject can tolerate without any know hazard. Clinical applicability must be demonstrated by performing numerous clinical trials of both systems.

## 5. ACKNOWLEDGMENTS

This work was supported by the SRC/ERC program (R11-2002-103) of MOST/KOSEF.

## 6. REFERENCES

Holder D. S., 2005, *Electrical Impedance Tomography: Methods, History and Applications*, IOP Publishing, Bristol, UK.

Lionheart W., Polydorides N., and Borsic A., 2005, The reconstruction problem in Holder D. S. (ed.), *Electrical Impedance Tomography: Methods, History and Applications*, IOP Publishing, Bristol, UK.

Oh T. I., Woo E. J., and Holder D. S., 2007, Multi-frequency EIT system with radially symmetric architecture: KHU Mark1, *Physiol. Meas.*, **28**, in press.

Woo E. J., Seo J. K., and Lee S. Y., 2005, Magnetic resonance electrical impedance tomography (MREIT) in Holder D. S. (ed.), *Electrical Impedance Tomography: Methods, History and Applications*, IOP Publishing, Bristol, UK.